

Direct Aerosol Synthesis of Large-Pore Amorphous Mesostructured Aluminosilicates with Superior Acid-Catalytic Properties**

Stéphanie Pega, Cédric Boissière, David Grosso, Thierry Azaïs, Alexandra Chaumonnot, and Clément Sanchez*

Making the best use of the petroleum resources still available is a necessity while alternative energy technologies mature. Thus, the conversion of heavy petroleum fractions into fuel is an important technological and economical challenge, especially to meet the needs for fuels.^[1] New refining catalysts are required, as the structured aluminosilicates commonly used are not optimum. The narrow pore size of zeolites is a limitation for the diffusion of heavy molecules, whereas the amorphous nature of mesostructured aluminosilicates reduces their potential activity (as a result of their moderate acidity) and hydrothermal resistance.

The quest for alternative large-pore acid catalysts has already led to the synthesis of very interesting aluminosilicates that combine mesostructured porosity with improved catalytic activity and hydrothermal resistance.^[2] In most cases, zeolite “seeds” are pre-formed in sodium ion-containing alkaline solution before they precipitate in presence of a surfactant. However, only long-chain-containing ammonium ions^[3] or amines^[4] can be directly used in basic media leading to maximum pore size of 3.5 nm. The use of amphiphilic block copolymers, such as [EO]_x-[PO]_y-[EO]_x pluronic P123 or F127, leads to larger pore sizes but necessitates a careful acidification step of the zeolite precursor. This acidification step favors interactions between silica and copolymer for the co-structure formation.^[6] The batch precipitation process, classically used for industrial production, can be significantly improved by eliminating the time-consuming and expensive steps such as separation, sodium ion exchange, or purification, which produces large volumes of solvent waste.

Herein we describe a new and efficient approach to design aluminosilicates for large-molecule cracking that takes into account not only the specific properties of the aluminosilicates with large pore mesostructures and higher acidity, but also optimizes the synthesis by use of the very attractive spray-drying process (see the Supporting Information). This

process strictly limits the number of steps in the synthesis before calcinations to two. The spray-dried solution was free of sodium ions and contains clear aluminosilicate precursors, pluronic F127 template, and tetrapropylammonium hydroxide (TPAOH) as the microstructure-directing agent (SDA). After atomization, the microdroplets are dried within the carrying gas, which induces a progressive concentration of non-volatile species. Eventually, suitable conditions are met so that polymer micelle self-assembly occurs as condensation of inorganic precursors takes place. The final mesostructured particles are then calcined to obtain the mesoporous particles.^[8] Such unique materials that are made of fully amorphous mesostructured spherical particles (pore diameters tuned between 6 and 17 nm) are called LAB (large-pore aluminosilicates made in basic media). Most importantly, the two-step synthetic procedure presented herein allows the precise control of Si/Al molar ratios from 6 to 50, as the Si/Al ratio fixed in the initial solution is preserved in the powder. The spray-drying process is advantageous compared to the precipitation approach as for the following reasons:

- 1) direct micellization and assembly of F127 in basic media without any acidification step;
- 2) a sodium-free medium (the materials are directly in the acidic form after the calcination step);
- 3) no zeolite “seed” preformation step is required (only hydrolysis of silicon and aluminum alkoxides is performed);
- 4) an industrially viable continuous and fast process (droplet to dry particle in 1–4 seconds);
- 5) the dry powder is collected directly on a filter.

Furthermore, some of the mesostructured aluminosilicates have higher catalytic activities with much lower coke formation for the *m*-xylene isomerization process than a 10 wt % Y-zeolite industrial reference. These characteristics of the catalyst were envisioned sixteen years ago with the MCM-41 family.

LAB materials were prepared as detailed in the Experimental Section. Figure 1 shows TEM pictures and corresponding low-angle XRD diagrams of samples containing various proportions of aluminum (2–14 molar %).

In all cases, the porosity is homogeneous throughout the sample, which is corroborated by the presence of a unique and fairly narrow correlation peak observed by low angle XRD (insets on TEM pictures, Figure 1). Such a short range periodicity is characteristic of worm-like organization of pores. Pore sizes were evaluated from N₂ adsorption isotherms (see Supporting Information) and range from 6 to 17 nm, depending on the aluminum and tetrapropylammo-

[*] Dr. S. Pega, Dr. C. Boissière, D. Grosso, T. Azaïs, Dr. C. Sanchez
Laboratoire de Chimie de la Matière Condensée de Paris, UPMC-
CNRS UMR7574
4 place Jussieu, CC 174, 75252 Paris Cedex 05 (France)
E-mail: clement.sanchez@upmc.fr

Dr. A. Chaumonnot
IFP-Lyon
Rond-point de l'échangeur de Solaize, 69390 Vernaison (France)

[**] TRAPDOR experiments were made through the TGIR RMN very-high-field program—FR 3050 CNRS. Dr. Pierre Florian (CEMHTI—UPR 3079 CNRS in Orléans, France) is greatly acknowledged for technical assistance with NMR and fruitful scientific discussions.

Supporting information for this article is available on the WWW under <http://dx.doi.org/10.1002/anie.200805217>.

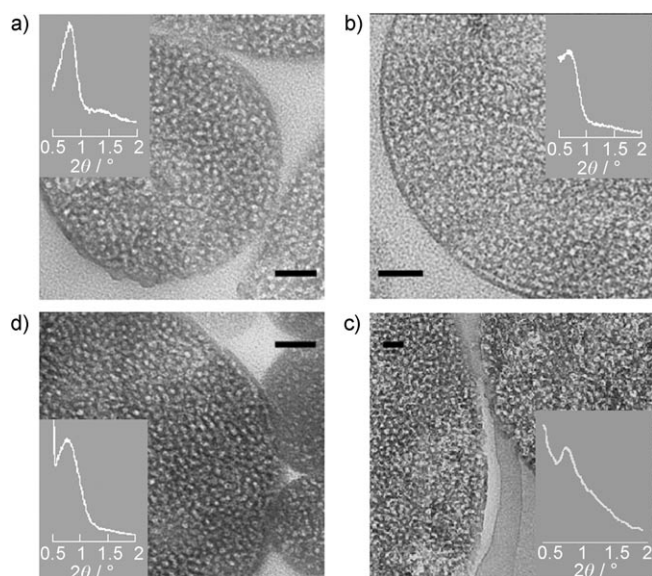


Figure 1. TEM images of a) 2%-LAB, b) 4%-LAB, c) 4%-LABo-3d, and d) 14%-LAB micro-atomized samples. Scale bars: 50 nm. Insets: Small-angle XRD patterns of the corresponding sample.

nium ion contents (Table 1) as expected, when F127 micellar templates are used. This observation confirms that the micellization and self-assembly occurred between the aluminosilicate phase and the F127 copolymer at pH of up to 11. This micellization and self-assembly was never reported before at a high pH value. The concomitant use of an evaporation process and tetrapropylammonium ions is probably responsible for the organic–inorganic interaction allowing the cooperative assembly. Furthermore, as a general trend, the mean pore size could be adjusted for a fixed

Table 1: Textural data of LAB samples and reference materials determined from N_2 adsorption isotherms.

Sample	Surface area [$m^2 g^{-1}$]	Microporous volume ^[a] [$m^3 g^{-1}$]	Pore volume [$cm^3 g^{-1}$]	Pore diameter ^[b] [nm]
2%-LAB	802	0.10	0.76	8.7
4%-LAB	779	0.12	0.71	8.6
4%-LABo-3d	748	0.16	0.84	15
4%-LABo-7d	712	0.15	0.81	15
4%-LABo-17d	761	0.20	0.62	15
4%-LABo-24d	734	0.21	0.62	26
8%-LAB-1	587	0.06	0.52	7.2
8%-LAB-2	553	0.08	0.53	8.2
8%-LAB-3	282	0.07	0.46	17
10%-LAB	330	0.04	0.41	11
14%-LAB	240	0.01	0.27	6.3
4%-SBA-15 ^[c]	881	0.09	1.07	10.3
8%-SBA-15 ^[c]	739	0.05	1.23	10.9
7%-Grace ^[d]	457	0.01	0.94	–
10%-Y/ Al_2O_3 ^[e]	298	0.02	0.65	–

[a] From α plot with LiChristopher non-porous silica reference. [b] Boekhoff–De Boer pore size distribution of N_2 adsorption curve. [c] Al-SBA-15 reference materials with 4% and 8% Al contents (from Ref. [7]). [d] Commercial amorphous aluminosilicate Grace 94 with Al content of 7%. [e] 10 wt.% of Y-zeolite, with Al content of 6% diluted in Al_2O_3 .

proportion of aluminum just by increasing the TPAOH content in the synthesis solution (for example, the pore diameter varies from 7.2 to 17 nm for samples 8% LAB-1 to LAB-3; Table 1). This effect is partly due to the pH increase that slows the inorganic matrix condensation, and partly due to the increasing amount of the added tetrapropylammonium ions. The detailed formation mechanisms will be described in a full paper.

The catalytic activities of LAB samples were evaluated and compared to reference materials in *m*-xylene isomerization. Solids were activated in a fixed-bed tubular reactor at 350 °C in dry air and then submitted to a flow (0.01 $mL min^{-1}$) of *m*-xylene. The reaction products were analyzed using gas chromatography in steps of 15 minutes. From the data given in Table 2, it appears that the 4%-LAB and 8%-LAB

Table 2: Catalytic activities measured for the *m*-xylene isomerization reaction.

Sample	Iso-weight activity ^[a] [$mmol h^{-1} g^{-1}$]	Iso-surface activity ^[b] [$\mu mol h^{-1} m^{-2}$]	Iso- S_{micro} activity ^[c] [$\mu mol h^{-1} m^{-2}$]
2%-LAB	0.78	0.97	2.91
4%-LAB	2.34	3.01	7.21
4%-LABo-3d	2.90	3.90	7.15
4%-LABo-5d	2.88	4.04	7.53
4%-LABo-17d	3.09	4.07	6.58
4%-LABo-24d	3.17	4.32	6.43
4%-SBA-15 ^[d]	1.32	1.50	4.64
8%-LAB-1	3.12	4.91	14.43
8%-LAB-2	3.48	6.29	16.72
8%-LAB-3	3.61	8.77	12.81
8%-SBA-15 ^[d]	1.65	2.24	9.05
7%-Grace ^[d]	0.42	0.92	–
6%-Y/ Al_2O_3 ^[d]	2.64	8.64	31.78
10%-LAB	2.35	6.71	16.47

[a] Obtained 10 min after starting the catalytic test. [b] Normalized with respect to the surface area. [c] Normalized with respect to the microporous surface. [d] Identical materials are described in Table 1.

samples exhibit nearly twice as much iso-weight activities compared to the Al-SBA-15 reference with the same aluminum content. The highest activities were obtained for the three 8%-LAB samples that are even strikingly more active than our 6%-Y-zeolite based reference material made of 10 wt.% percent of zeolite Y on Al_2O_3 . Moreover, the study of the *m*-xylene conversion versus time on-stream (Figure 2) shows that LAB materials are much less susceptible to deactivation by coke formation than the 10%-Y/ Al_2O_3 reference sample. This effect could be attributed to their larger pore size, but also to a milder acidity compared to Y zeolite. By looking at iso-surface activities, 8%-LAB samples are still much more active than the 8%-SBA-15 reference (Table 2), showing that LAB materials probably bear acidic sites stronger than those of “classical” amorphous aluminosilicates. Such specific acid sites could be obtained owing to the presence of tetrapropylammonium ion in the synthesis media, promoting local zeolite-like microstructure. However, inorganic networks of these materials have amorphous characteristics: no diffraction peak was observed at

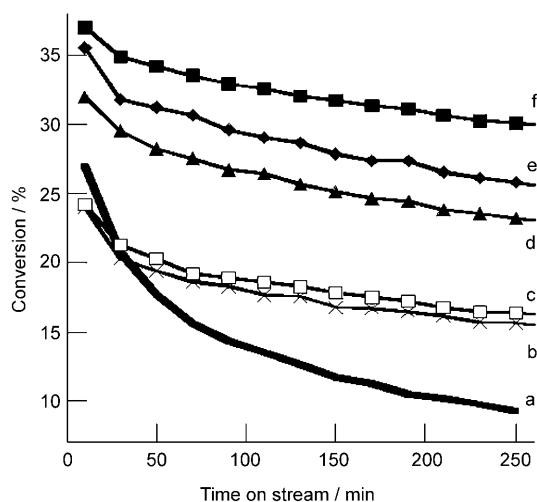


Figure 2. *m*-xylene conversion as function of the time on stream for a) 6%-Y/Al₂O₃ (Y-Zeolite-based industrial reference catalyst), b) 4%-LAB-1, c) 10%-LAB, d) 8%-LAB-1, e) 8%-LAB-2, and f) 8%-LAB-3 samples.

high angle in XRD, and the characteristic FTIR signature of ZMS-5 zeolite was not observed (five-membered ring vibration at 550 cm⁻¹). On the other hand, echo MAS ¹H NMR spectrum performed on dehydrated samples (same conditions as for catalytic test) exhibited unambiguous resonances at a chemical shift of around 4–5 ppm, similar to those of zeolitic Si-(OH)-Al acid sites^[9] and submitted to a [²⁷Al]-¹H TRAPDOR effect that shows the proximity between these protons and aluminum centers (see Supporting Information). The presence of such “zeolitic” protons could explain the high acidity of the LABs (Figure 3). The other resonances can be assigned using the [²⁷Al]-¹H TRAPDOR experiment. In particular, a broad band observed at higher chemical shift (δ = 6–9 ppm) submitted to a strong TRAPDOR effect can be attributed to protons in very close vicinity of aluminum centers and are engaged in hydrogen bonding with the

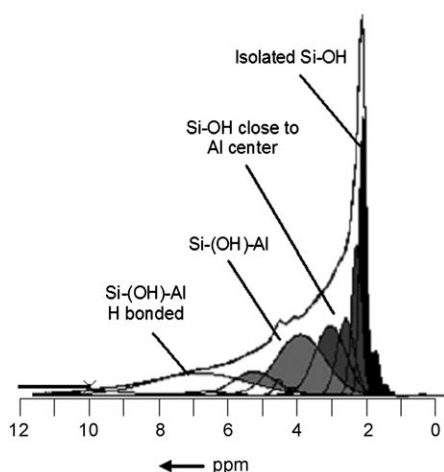


Figure 3. Echo MAS ¹H NMR spectrum of 8%-LAB-1 sample dehydrated at 200 °C. The chemical shift assignments are based on ²⁷Al-¹H TRAPDOR experiments (Supporting Information).

surrounding inorganic network (unlike the OH groups of a MFI zeolite nanobrick).

The Al–O–Si networks in the LABs are both completely amorphous and have strong Brønsted acidity similar to that observed for improved mesostructured materials prepared from zeolite seeds.^[2–5] This result is in contradiction with many previous works, which assume that, whether spontaneously formed at ambient temperature^[3] or promoted by pre-heating the zeolitic solution,^[2,4,5] zeolite seeds are needed to obtain strong acidity.

We prepared further materials, called LABo (“o” indicates old solutions), by following the same procedure, except that the solution containing the precursor was pre-treated at 80 °C for various times. Such additional conditioning is aimed at nucleating pre-zeolitic precursors (see Experimental Section). As examples TEM and low-angle XRD of 4%-LABo-3d are shown in Figure 1c. XRD patterns, and FTIR spectra of the corresponding 4%-LABo materials are available in the Supporting Information. For the longest pre-treatment times (17 and 24 days), nanocrystals of MFI zeolite were embedded in the mesoporous spheres. All the 4%-LABo materials are well-mesostructured, have the same aluminum content, and have similar specific surface areas (750 ± 20 m² g⁻¹). They develop additional microporous surface when the heating time during the pre-treatment increases (Table 1). The pre-heating is beneficial to sample properties as iso-weight catalytic activities of a 4%-LABo-3d (treated for 3 days) and LABo-5d (treated for 5 days) are improved by 24% compared with 4%-LAB sample. As these materials present similar surface areas, we could plot their iso-weight catalytic activity versus their microporous surface. A positive linear correlation between both was observed, indicating that *m*-xylene isomerization takes place preferentially in the micropores (Figure 4). We studied this hypothesis by trying to correlate the catalytic activity of all the LAB materials made so far with the number of weak, medium, and strong acid sites they bear. These were quantified by saturating the solids surface with 2,6-dimethylpyridine (2,6-DMP) followed by their thermodesorption, which was monitored by FTIR. No correlation could be found when the data were normalized

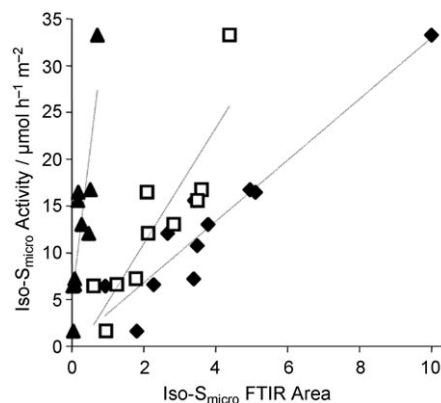


Figure 4. Catalytic activity of LAB materials versus relative number of (♦) strong + medium + weak, (□) strong + medium, and (▲) strong Brønsted acid sites. All data are normalized with respect to the microporous area of the solids

either by the weight or the surface area of the solids. On the contrary, when normalized by the microporous surface, a linear correlation was found (Figure 4). As a consequence, the microporous surface of LAB materials seems to be a relevant structural parameter to be considered to describe their catalytic properties in *m*-xylene isomerization. Considering this new parameter, the comparison of 8%-LAB material activity with reference materials at the same microporous surface (Table 2), confirms that the strength of their active acid sites is indeed higher than in classical amorphous aluminosilicates (8%-SBA-15 sample), whereas it seems to be much lower than in Y-zeolite (6%-Y/Al₂O₃ sample).

To summarize, the aerosol preparation of LAB materials is very attractive, as this process allows the direct production of tunable large pore size, high microporous volume, and high-surface-area mesostructured materials using XRD, FTIR, and NMR techniques. The complementary methods present superior acidity in the amorphous walls of the materials. This property is in complete contradiction with the usual assumption that the enhanced acidity of materials prepared in zeolitic pH range has its origin in the presence of zeolitic seeds. Their hydrothermal stability and their catalytic activity over large molecules are currently investigated to determine their potential application as commercial hydrocracking catalysts.

Experimental Section

Solutions of the precursors were prepared by first dissolving aluminum tri-*sec*-butoxide (ASB) in tetrapropylammonium hydroxide (TPAOH) solution (40% in water). Tetraethoxysilane (TEOS) was then added to the solution. After 16 h of stirring at room temperature, this solution (A) was mixed with a solution (B) of pluronic F127 in water and ethanol. The final molar composition was 1-*x*, *x*, *y*, 0.005, 57, 20 of Si, ASB, TPAOH, F127, H₂O, EtOH with $0 \leq x \leq 0.14$ and $0.15 \leq y \leq 0.23$. The solution was sprayed by a 6-Jet 9306A atomizer from TSI with an air pressure of 0.55 bar, and the aerosol was dried by passing through a quartz reactor heated at 350 °C. The powder obtained was treated at 90 °C overnight and then calcined at 550 °C for 8 h. The 2%-LAB and 4%-LAB materials were obtained for *x* = 0.02, *y* = 0.15, and *x* = 0.04, *y* = 0.17, respectively. The 8%-LAB materials were obtained for *x* = 0.08, with *y* = 0.17, 0.19, and 0.23 for 8%-LAB-1 to 8%-LAB-3 respectively. The 10%-LAB and 14%-LAB materials were respectively obtained for *x* = 0.10 and

0.14, with *y* = 0.21 for both. Materials were obtained with *x* = 0.04 and *y* = 0.17 by heating solution A, which was previously mixed with solution B, in propylene oxide bottle at 80 °C for 3, 7, 17, and 24 days (4%-LABo-3d, 7d, 17d, and 24d). An echo MAS ¹H NMR spectrum was recorded on a 750 MHz Bruker AV spectrophotometer with a spinning frequency of 33.3 kHz, and referenced with tetramethylsilane ($\delta(^1\text{H}) = 0$ ppm). TEM images were recorded on a Philips CM-12 at 120 kV. XRD patterns were obtained with a Bruker D8. Quantification of total (strong + medium) and strong acid sites were obtained by determining the areas of the FTIR bands at 1630, 1640, and 1650 cm⁻¹ after desorption of 1,3-DMP for 1 h at 100 °C, 200 °C, and 300 °C.

See the Supporting Information for XRD, TEM, IRTF of 4%-LABo; ²⁷Al-¹H TRAPDOR NMR spectra of 8%-LAB-1; ²⁷Al NMR of 4%-LAB, 8%-LAB-1, 10%-LAB, and 14%-LAB and N₂ adsorption-desorption isotherms of LAB samples.

Received: October 24, 2008

Published online: March 5, 2009

Keywords: aluminosilicates · heterogeneous catalysis · self-assembly · spray drying · xylene

- [1] a) A. Corma, *Chem. Rev.* **1997**, 97, 2373; b) A. Corma, *J. Catal.* **2003**, 216, 298.
- [2] a) Y. Liu, T. J. Pinnavaia, *J. Mater. Chem.* **2002**, 12, 3179; b) F.-S. Xiao, *Catal. Survey Asia* **2004**, 8, 151.
- [3] A. Aerts et al., *Appl. Catal. A* **2004**, 257, 7.
- [4] a) K. S. Triantafyllidis, E. F. Iliopoulou, E. V. Antonakou, A. A. Lappas, H. Wang, T. J. Pinnavaia, *Microporous Mesoporous Mater.* **2007**, 99, 132; b) S. Zeng, J. Blanchard, M. Breyse, Y. Shi, X. Su, H. Nie, D. Li, *Appl. Catal. A* **2005**, 294, 59; c) Z. Zhang, Y. Han, F.-S. Xiao, S. Qiu, L. Zhu, R. Wang, Y. Yu, B. Zou, Y. Wang, H. Sun, D. Zhao, Y. Wei, *J. Am. Chem. Soc.* **2001**, 123, 5014.
- [5] S.-S. Kim, Y. Liu, T. J. Pinnavaia, *Microporous Mesoporous Mater.* **2001**, 44–45, 489.
- [6] a) Y. Han, F.-S. Xiao, W. Wu, Y. Sun, X. Meng, D. Li, S. Lin, F. Deng, X. Ai, *J. Phys. Chem. B* **2001**, 105, 7963; b) Y. Liu, T. J. Pinnavaia, *Chem. Mater.* **2002**, 14, 3.
- [7] Y. H. Yue, A. Gedeon, J. L. Bonardet, N. Melosh, J. B. D'Espino, J. Fraissard, *Chem. Commun.* **1999**, 1967.
- [8] a) C. J. Brinker, Y. Lu, A. Sellinger, H. Fan, *Adv. Mater.* **1999**, 11, 579; b) C. Boissière, D. Grosso, H. Amenitsch, A. Gibaud, A. Coupe, A. N. Baccile, C. Sanchez, *Chem. Commun.* **2003**, 2798.
- [9] H. Liu, H.-M. Kao, C. P. Grey, *J. Phys. Chem. B* **1999**, 103, 4786.